Supplementary figures:

Figure S1. Normalized amplitude distribution of selected layer lines from Type 1 tubes of Bor1p. Each plot represents a different layer line, indicated by the Miller indices at the top. Subplots contain (1) the incoherent sum of power spectra generated with SPARX (continuous gray line), (2) the incoherent sum of extracted layer lines using the MRC suite (continuous black line), and (3-4) data from two different individual images with right and left sides of the meridian shown with dashed and dotted lines, respectively. The vertical dashed line represents the calculated radial position for the rising edge of the first peak assuming the (-10, 8) indexing scheme and r_{ctf} = 213 Å. For (-8, 7) the peak would be shifted to the left and for (-12,11) it would be shifted to the right.

Figure S2. Comparison of layer line data from Type 1 and Type 2 tubes. The black traces are from Type 1 tubes and grey traces from Type 2 tubes. The Miller index of each layer line is shown on the upper left and the corresponding Bessel orders are shown on the upper right. Note the expected shifts in the position of the initial peaks along the layer lines. Note also that although the Bessel order for the (1,0) layer line is -10 in both cases, the slightly larger diameter of Type 1 tubes means that the peaks are shifted slightly to the left (see equation 1).

Figure S3. Images of OmpF helical crystals. (A) Image of a collapsed tube in negative stain. The scale bar corresponds to 100 nm. (B) Fourier transform with unit cell vectors corresponding to the (1,0) and (0,1) reflections (blue and green, respectively). (C) Image of a frozen-hydrated OmpF tube. The scale bar corresponds to 100 nm. (D) Diffraction pattern and associated Miller indices (h,k) for layer lines from the frozen-hydrated OmpF tube with Miller indices indicated in the margins.

Figure S4. Analysis of the helical lattice for three different tubular crystals of OmpF. (A) The surface lattice corresponds to the unit cell parameters measured from the flattened tube in Fig. S3, with *a*, *b*, and γ equal to 129.5 Å, 129.9 Å and 60°. This same lattice is also plotted in C and E. The star indicates an arbitrary origin and the diamond, triangle and square correspond to circumferential vectors for three candidate schemes for the first OmpF tube, which were identified from origin refinement phase residuals (see text for candidate schemes). Black arcs indicate the circumference corresponding to the inner and outer leaflets of the membrane based on the mean radial density distrubtion from this first tube. (B) Reorientation and delimitation of the lattice to represent the helical net for the best indexing scheme. Helical families associated with (1,0) and (0,1) reflections are shown; the start numbers for these helical families correspond to the Bessel orders of the relevant layer lines. Two values for the circumference are listed, corresponding to that calculated from the drawing in A and that measured from the projected frozen-hydrated image using the mean radial density. (C,D) The same analysis applied to the second OmpF tube, which has different candidate indexing schemes and a slightly different circumference. (E,F) The same analysis applied to the third OmpF tube.

Figure S5. Maps from an OmpF tubular crystal. Sections through helical reconstructions from a single OmpF tube (represented by surface plots in Fig. S4C & D, using three candidate indexing schemes. The unit cell is shown by blue (*a* axis) and green (*b* axis) arrows. An asymmetric unit with the expected three-fold symmetry is obtained only from the (-29,20) indexing scheme. Note that no symmetry has been enforced for the reconstruction, though the location of an approximate three-fold axis is indicated by a triangle and asterisks highlight the three-fold character of the asymmetric unit.

Figure S1

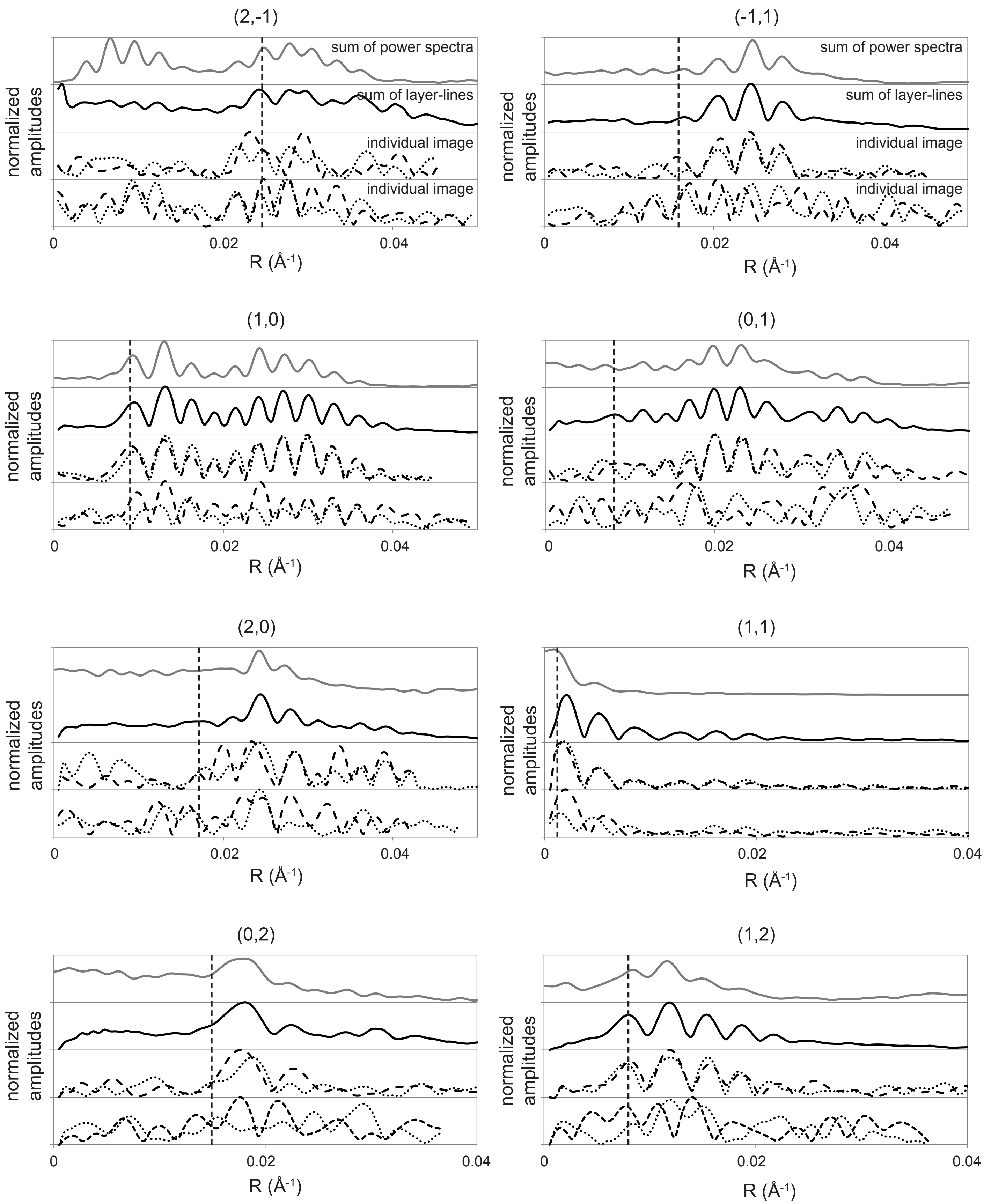
(2,-1)
(-1,1)
(1,0)
(0,1)
(2,0)
(1,1)
(0,2)
(1,2)
sum of power spectra
sum of layer-lines
individual image
individual image
normalized amplitudes
R (Å-1)
0
0.02
0.04

Figure S2

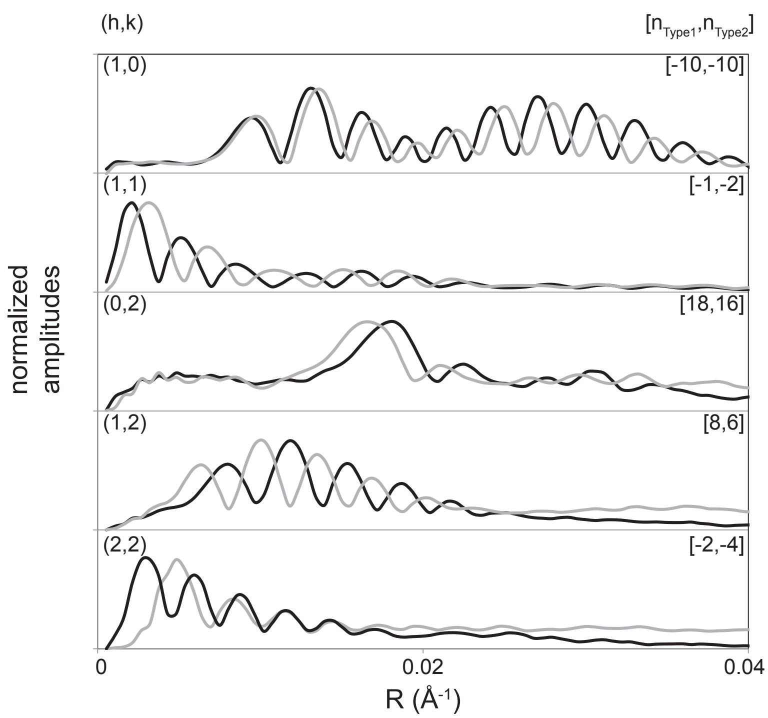

(h,k)
[n_{Type1},n_{Type2}]
(1,0)
[-10,-10]
(1,1)
[-1,-2]
(0,2)
[18,16]
(1,2)
[8,6]
(2,2)
[-2,-4]
normalized amplitudes
0
0.02
0.04
R (Å-1)

Figure S3

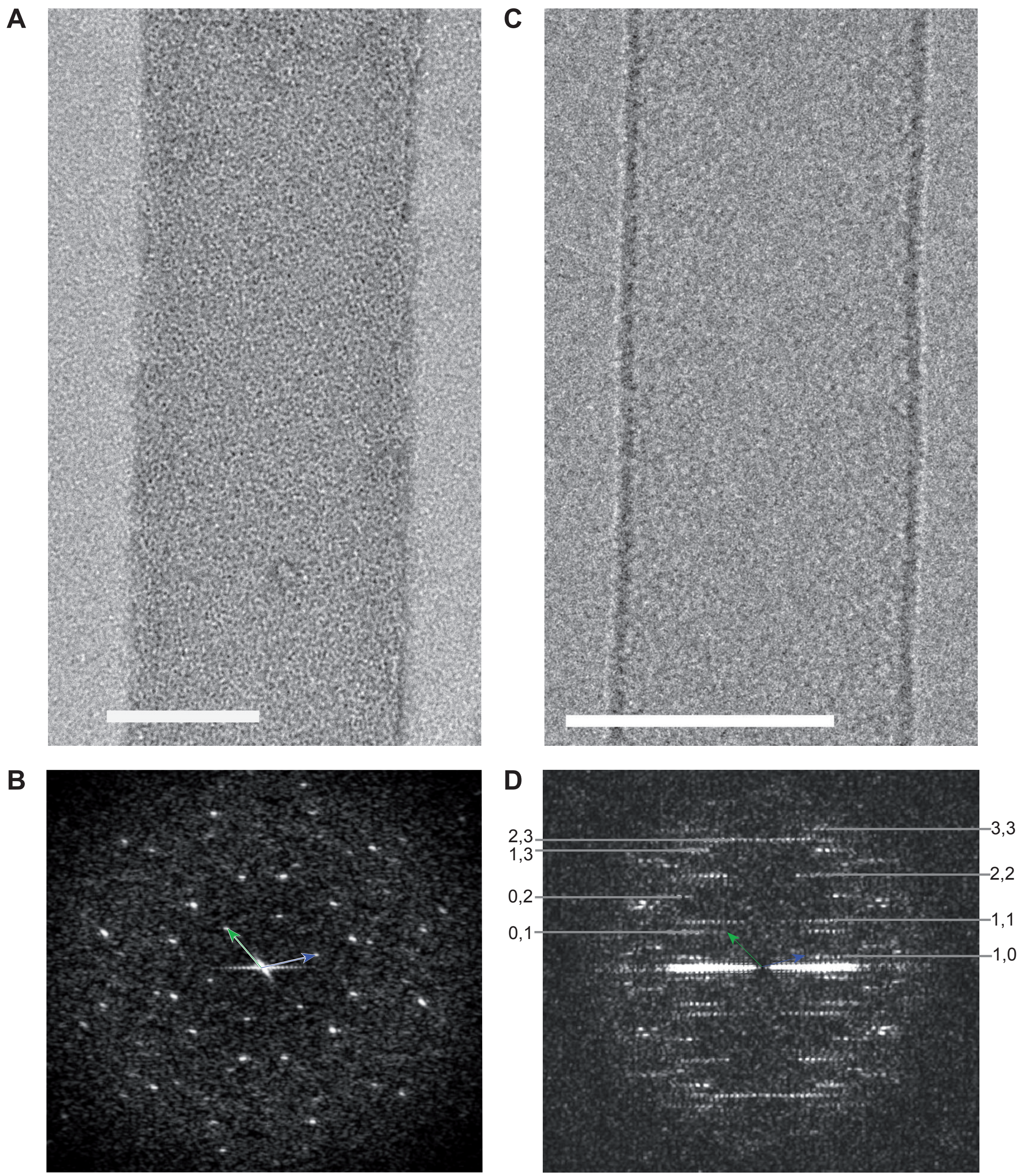

Figure S4

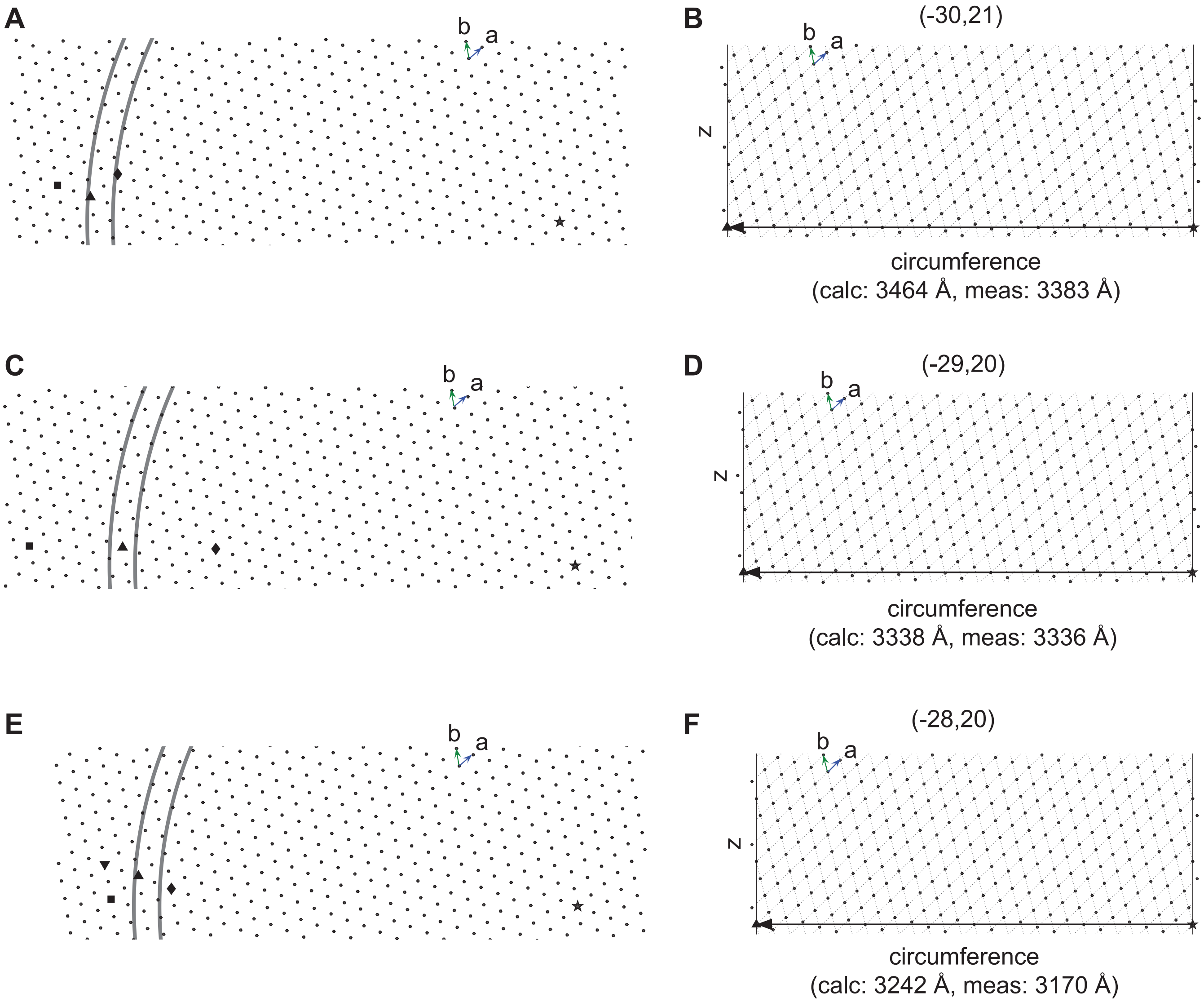
A
b
a
B
(-30,21)
b
a
z
circumference
(calc: 3464 Å, meas: 3383 Å)
C
b
a
D
(-29,20)
b
a
z
circumference
(calc: 3338 Å, meas: 3336 Å)
E
b
a
F
(-28,20)
b
a
z
circumference
(calc: 3242 Å, meas: 3170 Å)

Figure S5